Chemical Physics 539 (2020) 110978

Contents lists available at ScienceDirect

Chemical Physics

journal homepage: www.elsevier.com/locate/chemphys

Theoretical analysis of the spodium bonds in $HgCl_2$···L (L = ClR, SR_2, and PR_3) dimers

Tao Xia[1], Dan Li[1], Longjiu Cheng*

Department of Chemistry, Key Laboratory of Functional Inorganic Materials of Anhui Province, Anhui University Hefei, Anhui 230601, PR China

ARTICLE INFO

Keywords:
Spodium bond
Halogen bond
Non-covalent interaction
Density functional theory

ABSTRACT

Halogen bonds have received increasing interest in non-covalent interactions. Recently, a new kind of non-covalent interaction, spodium bond, was proposed to refer to a net attractive interaction between any element of group 12 and electron rich atoms. Due to strong relativistic effect, Hg is much different from the other group 12 elements, which prefers more linear coordination. Thus, we theoretically studied the model of $HgCl_2$···L (where L = ClR, SR_2, PR_3 families) to explore the nature of the linear coordinated spodium bonds. Analyses of electrostatic potential surfaces, together with ELF, LOL, and chemical bonding analyses, suggest the presence of covalent interaction. Complexes with nitrogen, oxygen, and fluorine donors result in more coulombic component, whereas others are dominated by covalent interaction, indicating coexistence of coulombic and covalent interaction. Besides, covalent interaction is significantly stronger with phosphorus donor. This model can provide intriguing perspectives for future weak intermolecular interactions studies.

1. Introduction

In recent years, weak intermolecular interactions represented by halogen bond (XB) have become a research hotspot [1–11]. It is the first non-covalent bond [12–19] found after hydrogen bond [20–26]. Due to the σ-hole, there can be localized regions of positive potential on halogen atoms, and halogen bond can be defined as a rather strong, directional, non-covalent interaction of an electropositive halogen (X = Cl, Br, or I) and an electron donor species (L) [27–28]. In the general definition Y–X···L [27], the Lewis base (neutral or anionic) gives electron to the acceptor X (Lewis acid), which is covalently attached to atom Y (usually C, N or X). The distance between the halogen bond donor and acceptor atoms (X···L) is shorter than the sum of their van der Waals radii and the Y–X···L angle is approximately linear.

The formation of halogen bond can be explained in two ways: 1) There will be an area of positive electrostatic potential opposite the Y-X σ bond (Y is generally an electron-withdrawing group), which is called σ-hole. Moreover, this phenomenon also exists in the fifth and sixth columns of the periodic Table 2) The anisotropy of electron density distribution around the covalent halogen atom makes the van der Waals radius of the halogen atom shorter in the Y-X bond direction and longer in the perpendicular direction. The anisotropy leaves a deficiency in the Y—X bond direction, and the halogen atoms can attract electron-rich groups to the maximum extent in the region of electron deficiency, making the halogen bond being in close to a straight line. Because of the anisotropy of the electrostatic potential distribution, halogen atoms have both electrophilic and nucleophilic properties.

Just as the elements of the halogen family (Cl, Br, I, etc) can replace hydrogen as a bridging atom in strongly bound complexes, the same is equally true for other columns of the periodic table. In particular, the S group can engage in chalcogen bond [29–35], and the same is true of the P family which forms pnicogen bond [36–39].

Though studied for decades, the nature of these kinds of interaction to date suffers from controversy. The forces involved in the formation of the halogen bond have been described as primarily coulombic interactions [12,40–43]. However, coulombic interactions cannot play the sole role, and other interactions, such as polarization [17,44–46], charge transfer [47–50] and dispersion [51] should not be negligible [2,52]. Apart from these interactions, are there any other patterns?

Recently, Antonio bauzá et al. proposed a new non-covalent interaction, spodium bond, to refer to a net attractive interaction between any element of group 12 and electron rich atoms [53]. In SpX_2L_2 (Sp = Zn, Cd, Hg) compounds, the coordination bonds (classical ligand–Metal bond) and non-covalent interactions were differentiated by the term spodium bond. However, only the four-coordinated Sp atoms were concerned in that work. Due to strong relativistic effect, Hg is

* Corresponding author.
E-mail address: clj@ustc.edu (L. Cheng).
[1] These two authors contribute equally to this work.

https://doi.org/10.1016/j.chemphys.2020.110978
Received 27 July 2020; Received in revised form 22 August 2020; Accepted 30 August 2020
Available online 04 September 2020

much different from the other group 12 elements, which prefers more linear coordination in sp hybridization, e.g., cinnabar (hexagonal, red HgS) [54] and $(HgS)_n$ clusters [55]. There should also be similar spodium bonds between linear coordinated Hg atom and the electron rich atoms. The S···Hg secondary bonding networks in $(HgS)_n$ clusters suggested in our previous work should be taken as spodium bond in definition [55].

To give a systematic study on spodium bond of linear coordinated Hg atom, this work theoretically investigated the $HgCl_2$···L (L = ClR, SR_2, PR_3 families) dimers. $HgCl_2$ is a well-known linear molecule in chemistry books at the high schools, which is soluble in water but is difficult to be ionized. In this molecule, a large positive electrostatic potential is generated on the waist of Hg atom. Thus, there should be strong attraction between Hg and an electron donor species (Hg···L), and Hg···O spodium bonds may result in high solubility of $HgCl_2$ in water. On the other hand, with an electron donor species, the linearity of $HgCl_2$ molecule is broken a tittle. Hybridization of Hg atom should have certain sp^2 character, and the Hg···L interaction should have some character of coordination bond. Therefore, both coulombic (spodium bond) and covalent (coordination bond) components are important in $HgCl_2$···L dimer. In this study, taking $HgCl_2$···L (L = ClR, SR_2, PR_3 families) dimers as test cases, we theoretically studied the trend of contributions of coulombic and covalent interactions, uncovering the nature of these kinds of weak intermolecular interactions.

2. Computational methods

The geometric structures are optimized by density functional theory (DFT) at the M06-2X [56]/def2-TZVPP level. All structures are verified as true minima by frequency check. All DFT calculations are carried out using the Gaussian09 package [57]. Natural bond orbital (NBO) [58–60] analysis is performed for all complexes using the Gaussian09 NBO module at the same level of theory. The binding energies of the dimers are calculated at the M06-2X/def2-QZVP and CCSD(T) [61]/def2-QZVP levels of theory with basis-set superposition error (BSSE) correction. The electron densities of the complexes are analyzed using the electron localization function (ELF) [62] and localized orbital locator (LOL) [63] methodology employing the Multiwfn package [64]. No-ncovalent interaction (NCI) [65] indexes are plotted by using Multiwfn and VMD [66] packages at the M06-2X/def2-TZVPP level. Chemical bonding analysis is employed by using the adaptive natural density partitioning (AdNDP) [67] method at the M06-2X/def2-TZVPP level. The molecular electrostatic potentials of the isolated monomers are represented on the 0.001 a.u. electron density isosurfaces. The energy decomposition analysis (EDA) [68] is conducted based on combining the extend transition state (ETS) [69,70] method with natural orbitals for chemical valence (NOVC) [71,72] theory as embedded in the Amsterdam density functional (ADF) [73] at the B3LYP-D3(BJ)/TZ2P level. EDA by the symmetry-adapted perturbation theory (SAPT) [74] is performed on PSI4 package [75] at the sapt2+(3)dmp2/def2-QZVP level.

3. Results and discussion

To give a systematic study of the interaction between $HgCl_2$ and ligands, the Cl, S, P families are considered. The ligands are ClR (R = CH_3) for Cl family (F, Cl, Br or I), SR_2 for S family (O, S, Se or Te), and PR_3 for P family (N, P, As or Sb).

3.1. L = Sr_2

The optimized structure of $HgCl_2$···H_2O dimer (**1**) is shown in Fig. 1a. The Cl-Hg-Cl angle is about 180° in the dimer, indicating *sp* hybridization of Hg. In the dimer, the natural charges of Hg and O are +1.02 and −0.95, respectively. The calculated Hg···O distance (2.739 Å) is obviously shorter than their sum of van de Waals radii

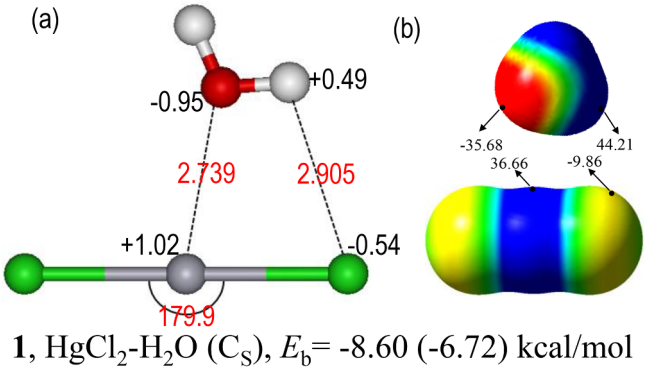

Fig. 1. (a) Optimized structure of $HgCl_2$···H_2O dimer, and (b) electrostatic potential surfaces of H_2O and $HgCl_2$. Red and blue regions refer to most negative and positive regions, respectively. Bond lengths (Å) and angle (degree) are given in red. Natural charges are labeled to the atoms. E_b gives the binding energy at the M06-2X/def2-QZVP (CCSD(T)/def2-QZVP) level. The minimal/maximal values (in kcal/mol) of electrostatic potential are also labeled.

(3.490 Å). Thus, there should be a strong attractive interaction between Hg···O. Apart from Hg···O interaction, H···Cl hydrogen bond is also involved in the dimer (Fig. 1a) according to the charges (+0.49 for H and −0.54 for Cl) and hydrogen-chlorine distance (2.905 Å). In addition, the electrostatic potential surfaces (Fig. 1b) clearly show the coulombic interactions of mercury with oxygen and hydrogen with chlorine. Though the calculated binding energy (−8.60 kcal/mol) is fairly large, it is difficult to measure the contribution of Hg···O interaction to the binding energy because of the influence of H···Cl hydrogen bond.

Thus, we replace H by CH_3 to avoid the influence of hydrogen bond. Fig. 2 plots the optimized structures of $HgCl_2$···$O(CH_3)_2$ (**2**), $HgCl_2$···$S(CH_3)_2$ (**3**), $HgCl_2$···$Se(CH_3)_2$ (**4**), and $HgCl_2$···$Te(CH_3)_2$ (**5**) dimers. $HgCl_2$ across different chalcogen ligands have all deviated from the original linear form, and the hybridization may be changed, gradually tending to sp^2 hybridization. The natural charge of the Hg atom is still + 1.02 for dimer **2** compared with that of dimer **1**, while the natural charge of the O atom has decreased to −0.54 with a higher binding energy (−10.64 kcal/mol). As can be seen from the figure, the negative charges in the donor atoms decrease from dimers **2** to **5**, where the minimal values of electrostatic potential change from −31.65 to −19.85 kcal/mol. However, the trend in binding energy (increasing from −10.64 to −11.69 kcal/mol) is exactly opposite to that of coulombic interactions from dimers **2** to **5**, indicating that there exists other interactions along with coulombic interaction, probably covalent interaction. The charge delocalizations of L → Hg also lead to the changes in the natural charges. The natural charge for oxygen in dimer **2** is negative (−0.54), whereas that in dimer **3** is positive (+0.25), and those in dimer **4** (+0.33) and dimer **5** (+0.51) are even more positive. Besides, the natural charges for Hg decrease with the order from O (+1.02) to Te (+0.89) donors. All these are indicative of lone pair electrons transferring from chalcogen elements to the vacant orbitals of Hg, resulting in Cl-Hg-Cl angle gradually deviating from 180°. The heavier the element is, the more the electrons transform, giving rise to more contribution of covalent interaction. Taken together, these calculations suggest the possibility and rationality of covalent interactions in these model.

3.2. L = Clr

Fig. 3 plots the optimized structures of $HgCl_2$···FCH_3 (**6**), $HgCl_2$···$ClCH_3$ (**7**), $HgCl_2$···$BrCH_3$ (**8**) and $HgCl_2$···ICH_3 (**9**) dimers. From dimers **6** to dimer **9,** the Cl-Hg-Cl angle reduced from 177.1° to 174.5°. This trend is consistent with $HgCl_2$···SR_2, gradually deviating from 180°, but Cl-Hg-Cl angles in Fig. 3 is bigger than the corresponding

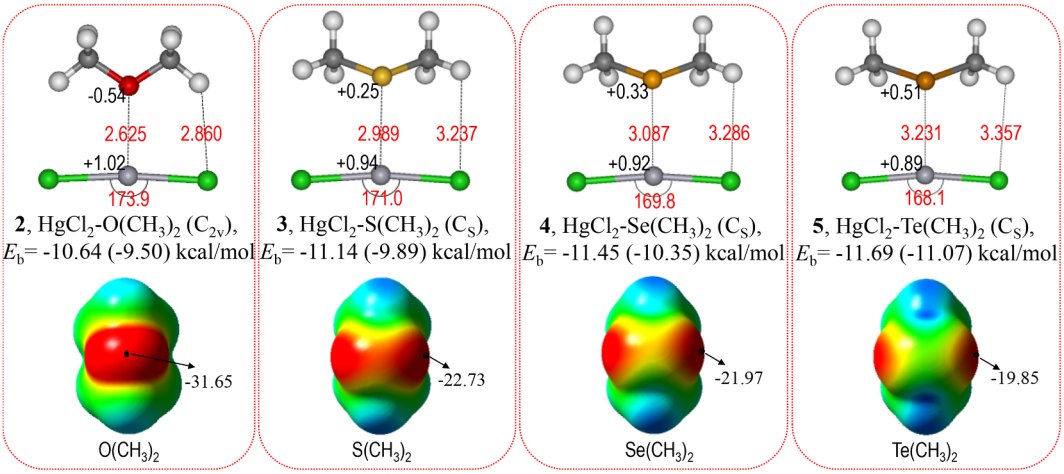

Fig. 2. Optimized structures of $HgCl_2\cdots SR_2$ dimers, and electrostatic potential surfaces of SR_2. Red and blue regions refer to most negative and positive regions, respectively. Bond lengths (Å) and angle (degree) are given in red. E_b gives the binding energy at the M06-2X/def2-QZVP (CCSD(T)/def2-QZVP) level. The minimal values (in kcal/mol) of electrostatic potential are also labeled.

angles in Fig. 2. It is obvious that the interaction between chalcogens and mercury is stronger than that between halogens (the same row as the corresponding chalcogens) and mercury with longer halogen-mercury distance. According to the changes of electrostatic potential and natural charge, similar to the results in S family, we can conclude that covalent components in Cl family are weaker, leading to the increasing binding energies from dimer **6** to dimer **9** in spite of the reduced coulombic interactions. Simultaneously, comparing the natural charges with SR_2, we come to the conclusion that the coulombic interaction between halogen and mercury should be stronger when L = ClR, but in fact, the trend in the binding energies is just opposite, which suggests that the covalent interactions between mercury and donor atom increase from the corresponding elements of groups 17–16.

3.3. L = Pr_3

Similarly, we have also done structural optimization of $HgCl_2\cdots PR_3$. Fig. 4 plots the optimized structures of $HgCl_2\cdots N(CH_3)_3$ (**10**), $HgCl_2\cdots P(CH_3)_3$ (**11**), $HgCl_2\cdots As(CH_3)_3$ (**12**), and $HgCl_2\cdots Sb(CH_3)_3$ (**13**) dimers. As discussed above, in groups 16 and 17 donor elements, binding energies of Hg···L dimers are larger with heavier donor atoms, indicating an increasing tendency of covalent components when the donor atom of L become heavier. However, elements of group 15 tell a different story. The deviation of Cl-Hg-Cl angles reach an extreme value in $HgCl_2\cdots P(CH_3)_3$ (160.8°). Electrostatic potential analysis shows that coulombic interaction in dimer **10** should be the strongest. However, from the bond angles and binding energies, the strongest Hg···L attraction occurs at dimer **11**. The natural charges of phosphorus (+0.87) and mercury (+0.89) indicate more electron transferring from phosphorus to the unoccupied orbital of mercury compared with the other donor atoms. This irregularity was previously detected for halogen bond interactions, which can be explained in terms of combination of rehybridisation and hyperconjugation [76]. It can be speculated that the covalent interaction of dimer **11** is the strongest among these dimers.

From groups 17 to 16, and to 15 elements, the Hg···L binding energies increase from right to left and from top to bottom according to the periodic table of elements, but phosphorus is an exception, involving the maximal binding energy, perhaps owing to the strongest covalent interaction among all these complexes.

3.4. NBO analyses

To unveil the nature of interaction in these complexes, NBO analysis was also performed at the M06-2X/def2-TZVPP level (Table 1).

In HgCl2···L dimers, the deviations of Cl-Hg-Cl angle are obviously smaller when L is ClR family, in good agreement with the change trend

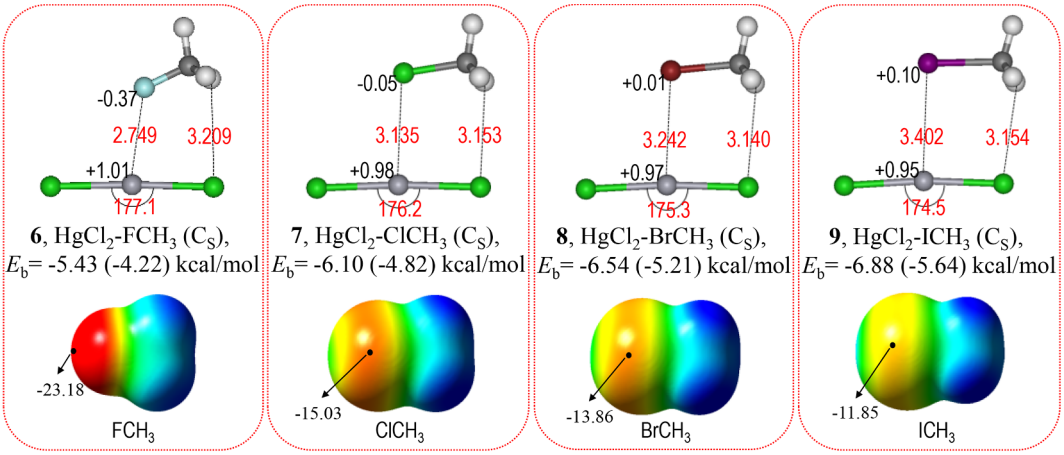

Fig. 3. Optimized structures of $HgCl_2\cdots ClR$ dimers, and electrostatic potential surfaces of ClR. Red and blue regions refer to most negative and positive regions, respectively. Bond lengths (Å) and angle (degree) are given in red. E_b gives the binding energy at the M06-2X/def2-QZVP (CCSD(T)/def2-QZVP) level. The minimal values (in kcal/mol) of electrostatic potential are also labeled.

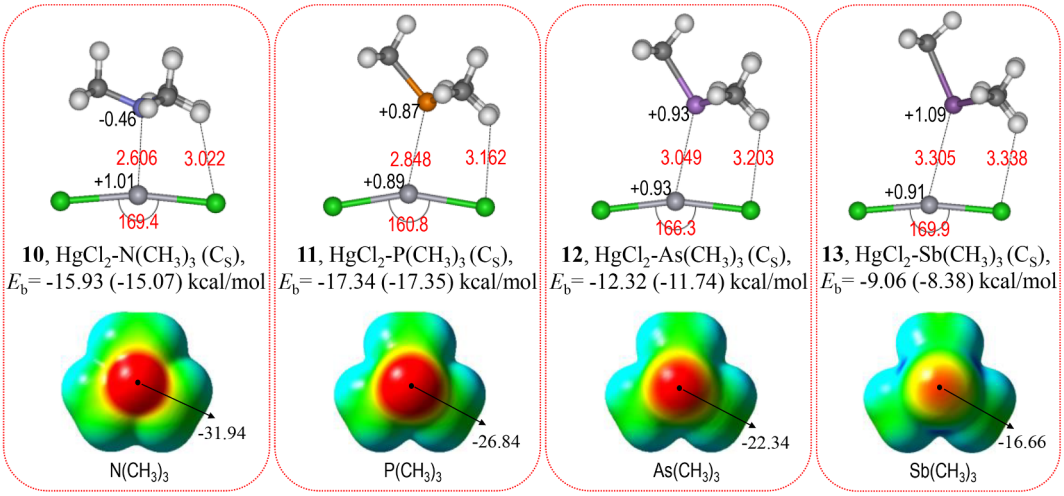

Fig. 4. Optimized structures of $HgCl_2\cdots PR_3$ dimers, and electrostatic potential surfaces of PR_3. Blue and red regions refer to most negative and positive regions, respectively. Bond lengths (Å) and angle (degree) are given in red. E_b gives the binding energy at the M06-2X/def2-QZVP (CCSD(T)/def2-QZVP) level. The minimal values (in kcal/mol) of electrostatic potential are also labeled.

Table 1
Deviation degree of Cl-Hg-Cl angle, orbital hybridization of Hg atom, and charge transfer from L to Hg at the M06-2X/def2-TZVPP level.

Complex	Angle[a]	Hybridization[b]	Charge L[c]	Charge Hg[d]
HgCl2···FCH_3	2.9°	$sp^{1.05}$	−0.02	+0.01
HgCl2···$ClCH_3$	3.8°	$sp^{1.04}$	+0.01	−0.02
HgCl2···$BrCH_3$	4.7°	$sp^{1.04}$	+0.02	−0.03
HgCl2···ICH_3	5.5°	$sp^{1.04}$	+0.04	−0.05
HgCl2···$O(CH_3)_2$	6.1°	$sp^{1.07}$	−0.04	+0.02
HgCl2···$S(CH_3)_2$	9.0°	$sp^{1.35}$	+0.05	−0.06
HgCl2···$Se(CH_3)_2$	10.2°	$sp^{1.36}$	+0.06	−0.08
HgCl2···$Te(CH_3)_2$	11.9°	$sp^{1.38}$	+0.10	−0.11
HgCl2···$N(CH_3)_3$	10.6°	$sp^{1.05}$	−0.03	+0.01
HgCl2···$P(CH_3)_3$	19.2°	$sp^{1.37}$	+0.10	−0.11
HgCl2···$As(CH_3)_3$	13.7°	$sp^{1.13}$	+0.03	−0.07
HgCl2···$Sb(CH_3)_3$	10.1°	$sp^{1.12}$	+0.06	−0.08

[a] The deviation degree of Cl-Hg-Cl angle from 180°. [b]Hybridization of Hg atom. [c]Charge changed of L atoms from monomers to dimers. [d]Charge changed of Hg atom from monomers to dimers.

Table 2
Decomposition of interaction energies (in kcal/mol) in $HgCl_2\cdots L$ dimer complexes at the B3LYP-D3(BJ)/TZ2P level.

Complex	E_{int}	E_{pauli}	E_{elst}	E_{oi}	E_{disp}
HgCl2···FCH_3	−4.54	10.62	−9.21	−3.16	−2.79
HgCl2···$ClCH_3$	−5.87	13.34	−10.27	−4.76	−4.17
HgCl2···$BrCH_3$	−6.68	15.07	−11.52	−5.65	−4.58
HgCl2···ICH_3	−7.29	17.32	−12.95	−6.52	−5.14
HgCl2···$O(CH_3)_2$	−9.87	22.87	−20.32	−7.66	−4.77
HgCl2···$S(CH_3)_2$	−11.92	30.18	−24.00	−11.54	−6.56
HgCl2···$Se(CH_3)_2$	−12.98	32.30	−25.92	−12.58	−6.79
HgCl2···$Te(CH_3)_2$	−13.86	36.28	−28.88	−14.12	−7.14
HgCl2···$N(CH_3)_3$	−16.08	42.11	−36.08	−14.29	−7.82
HgCl2···$P(CH_3)_3$	−19.38	57.80	−45.50	−21.96	−6.72
HgCl2···$As(CH_3)_3$	−13.55	36.09	−28.75	−14.71	−6.19
HgCl2···$Sb(CH_3)_3$	−10.39	28.28	−21.57	−11.18	−5.92

in hybridization. It can be concluded that larger deviation degree results from more electrons transferring from donor atom to the empty orbital of mercury, corresponding to the tendency from sp to sp^2 hybridization. In addition, it is shown that $HgCl_2\cdots P(CH_3)_3$ involves the largest deviation degree (19.2°) and the strongest covalent interaction.

When the donor atoms, such as fluorine, oxygen and nitrogen, form dimers with $HgCl_2$, electrons transfer from mercury to the donor atoms, which is favorable for coulombic interaction. By contrast, when other elements form dimers with $HgCl_2$, the electron transfer is from the donor atoms to the mercury atom, leading to covalent interaction. The more the electron transfer from the donor atoms to the vacant orbital of mercury, the more obvious tendency to sp^2 hybridization, all of which point to the existence of covalent interaction. The Hirshfeld and Mulliken charges (Table S1) were also calculated, which kept the same trend with the NBO charge.

3.5. ELF and LOL analyses

ELF (Electron Localization Function) analysis is a common method for describing chemical bonding in real space, and its function is very powerful. The value of ELF ranges from 0.0 to 1.0, where the relatively large values (0.5 to 1.0) indicate regions containing bonding and non-bonding localized electrons, whereas smaller values (< 0.5) describe regions where electron are expected to be delocalized. To further verify our conjecture, we use ELF (Fig. 5) to characterize it. It is clear that the color change in $HgCl_2\cdots P(CH_3)_3$ dimer is the most obvious, with the shortest Hg···L distance, showing the strongest covalent interaction among all the dimers.

The LOL (Localized orbital locator) diagram can also clearly and intuitively show the chemical structure and accurately identify the chemical bonding. Areas without electrons ($0.0 < LOL < 0.5$, plotted in light blue, blue and dark blue to represent fewer and fewer electrons in space), such as those far away from the nucleus and between the atomic shell, indicate that no covalent bond has been formed. The chemical content of LOL is similar to that of ELF, as both depend on the kinetic-energy density. However, LOL simply recognizes that gradients of localized orbitals are maximized when localized orbitals overlap, whereas ELF is founded on consideration of the electron pair density. In the $HgCl_2\cdots L$ dimers, the results of LOL analysis in Fig. 6 are very similar to those of ELF, covalent interactions existing and the strongest one lying in $HgCl_2\cdots P(CH_3)_3$ dimer.

3.6. NCI analyses

The contribution of H···Cl interaction may be large in the dimer, and it is very difficult to distinguish the contribution of H···Cl and L···Hg directly. Strength of the weak interactions can be given by non-covalent interactions (NCI) indexes based on the positions of the spikes. In dimers **2–13**, the H···Cl distance in dimer **2** is the shortest, and the interaction should be the strongest. Fig. 7 plots the NCI analysis of

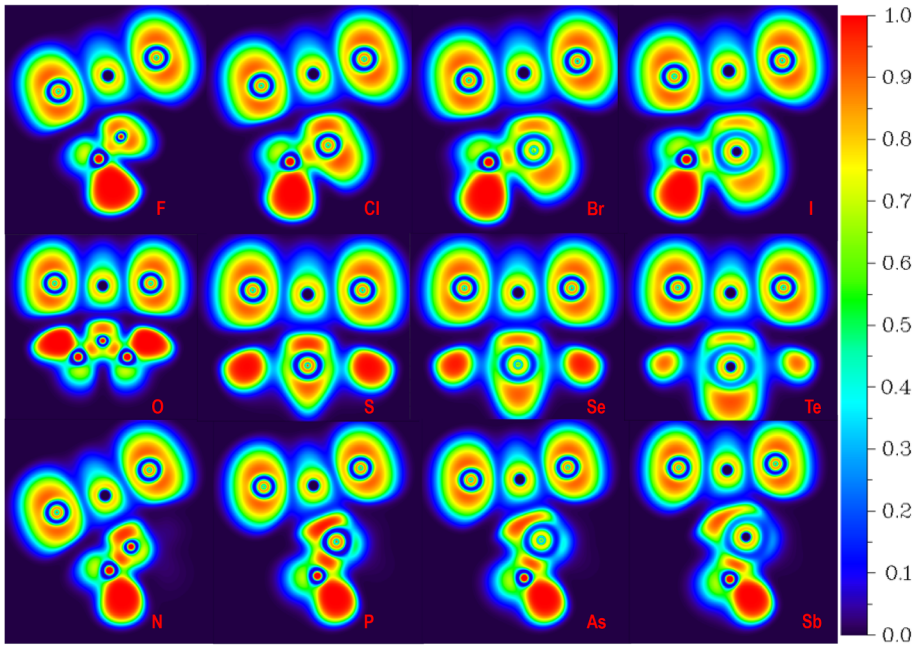

Fig. 5. ELF contour planes for dimers **2–13** (HgLC planes). Labeled is the color scale of the values.

dimer **2**. The H···Cl spike lies in −0.008, which is very weak and should be taken as van der waals interaction. However, the spike of O···Hg spodium bond lies in −0.030, which is rather strong and is a typical secondary interaction. Thus, the contribution of H···Cl interaction in the dimers should be very small compared to the spodium bonds. NCI analysis for the other dimers is also given in Fig. S1.

3.7. Chemical bonding analyses

To gain more direct insight into the nature of the bond in $HgCl_2$···L, we apply adaptive natural density partitioning (AdNDP) method to obtain patterns of chemical bonding. AdNDP is based on the concept of the electron pair as the main element of chemical bonding models, which allows an electron pair to be delocalized over more than two

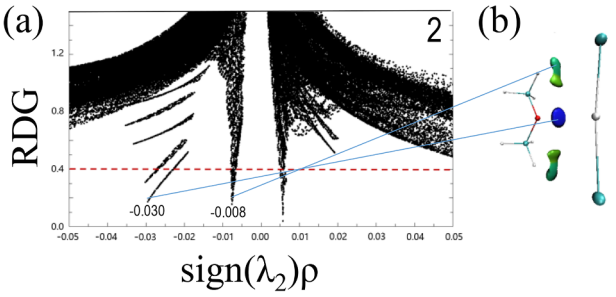

Fig. 7. Plots of the reduced density gradient (RDG in a.u.) against the sign of the second Hessian eigenvalue multiplied by the electron density (sign(λ_2)ρ in a.u.) for the dimers $HgCl_2$···$O(CH_3)_2$ (**2**), (a). NCI isosurfaces at s = 0.40 (b).

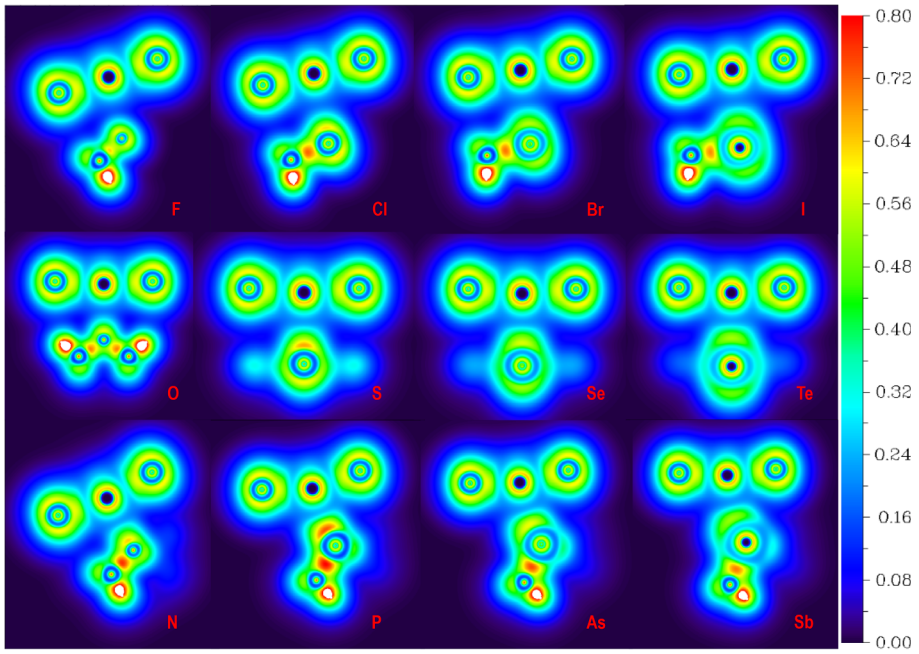

Fig. 6. LOL contour planes for dimers **2–13** (HgLC planes). Labeled is the color scale of the values.

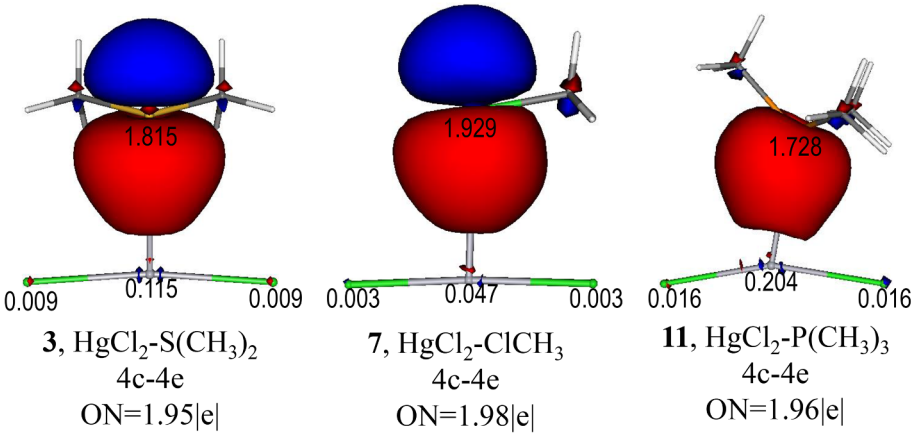

Fig. 8. AdNDP localized 4c-2e (LHgClCl) orbitals of dimers $HgCl_2\cdots S(CH_3)_2$ (**3**), $HgCl_2\cdots ClCH_3$ (**7**), and $HgCl_2\cdots P(CH_3)_3$ (**11**).

atoms. Fig. 8 displays the AdNDP localized bonds of dimers **3** ($HgCl_2\cdots S(CH_3)_2$), **7** ($HgCl_2\cdots ClCH_3$), and **11** ($HgCl_2\cdots P(CH_3)_3$). Since charge transfer in halogen bond have been extensively discussed in literatures, we consider the bonds in dimers **3**, **7** and **11** as 4c-2e bonds to include the contribution of $\sigma^*_{Hg\text{-}Cl}$ bond. The fact that the numbers of bonding orbitals occupied all close to the ideal value of 2.00|e| indicates high reliability. The phosphorus donor affords more electrons to mercury than sulfer or chlorine do, leading to more covalent interaction in dimer **11**. By contrast, electrons in dimer **7** mainly concentrate on chlorine, and the dominant interaction should be coulombic interaction. Besides, electrons are mostly focused on mercury and the donor atoms, while electrons that transfer to the $\sigma^*_{Hg\text{-}Cl}$ orbital are negligible, indicating that coulombic and covalent interactions rather than charge transfer dominate intermolecular interactions in the dimers.

3.8. Energy decomposition analyses

Energy decomposition analysis is another tool to understand the nature of intermolecular interactions at the energy level. To investigate which one is the main driving force for the formation of intermolecular interactions in selected complexes. The total binding energy (E_{int}) is decomposed into four terms: Pauli repulsion energy (E_{pauli}), electrostatic interaction energy (E_{elst}), orbital interaction energy (E_{oi}) and dispersion energy (E_{disp}). The results are listed in Table 2. As shown in Table 2, the E_{elst}, E_{oi} and E_{disp} are negative values which denote attractive interactions, that is, they make a contribution to stabilize the formation of $HgCl_2\cdots L$ dimer complexes. However E_{pauli} is positive, meaning that it is a repulsive interaction and makes a contribution to destabilize the formation of the complexes. The largest attractive contribution to the formation of the $HgCl_2\cdots L$ dimer complexes results from E_{elst}, followed by E_{oi} and E_{disp}, the E_{oi} being approximately a half of the E_{elst}. Therefore, the larger E_{oi} value demonstrates that the orbitals undergo obvious changes in the formation of the complexes. In the conceptual Kohn–Sham framework, the E_{oi} term accounts basically for charge-transfer and donor–acceptor orbital interactions between the two fragments, and can be considered as a measure of the covalent character of the intermolecular bond. The bigger contribution of the E_{oi} in $HgCl_2\cdots L$ dimers indicates the higher covalence of the formed bonding. Similarly, $HgCl2\cdots P(CH_3)_3$ dimer involves the strongest covalent interaction.

There were previously some studies suggesting such ETS-NOCV-EDA schemes may overestimate the covalent contribution [77,78]. Thus, EDA results by SAPT method are also given for reference (Table S2). The total binding energies and Pauli repulsion energies of SAPT are in good agreement with those of ETS-NOCV-EDA. However, electrostatic interaction energies in SAPT is obviously less negative and dispersion energies in SAPT are more negative. Orbital interaction energies in SAPT are smaller a little, but is also fairly large (−16.28 kcal/mol for dimer **11**).

As discussed above, although Sp bonds in $HgCl_2\cdots L$ complexes should be classified in noncovalent interactions by Hg···L distances and interaction energy, the contribution of covalent interaction is non-negligible (E_{oi} being approximately a half of the E_{elst}), which is in disagreement with the noncovalent interaction in $HgCl_2L_2\cdots L$ in ref. 53. In $HgCl_2$ molecule, Hg atom is in sp hybridization with empty $6p_x$ and $6p_y$ orbitals, and the Hg···L Sp bond can have certain character of L → Hg coordination bond. The coordination character is especially large for $L = P(CH_3)_3$, where the interaction energy is about a half the traditional coordination bond in L_3P-CuX [79]. However, in $HgCl_2L_2$ molecule, Hg atom is in sp^3 hybridization, and there is no room for L → Hg covalency in $HgCl_2L_2\cdots L$ Sp bond.

3.9. $HgCl_2\cdots L_n$ complexes ($L = O(CH_3)_2$ and $S(CH_3)_2$)

As shown in Fig. 1, there is a large positive electrostatic potential on the waist of Hg, so one $HgCl_2$ molecule may form several spodium bonds around the waist. Taking $O(CH_3)_2$ and $S(CH_3)_2$ as the test cases, we optimized the structures of $HgCl_2\cdots L_n$ complexes at the M06-2x/def2qzvp level of theory. Fig. 9 plots the structures and ΔH_n (kcal/mol) as the function of coordination number (n), where $\Delta H_n = E(HgCl_2\cdots L_n) - E(HgCl_2\cdots L_{n-1}) - E(L)$. For $L = O(CH_3)_2$, ΔH_n is very large for n = 1–5 (-9 ~ -11 kcal/mol), and there is a sudden decrease of ΔH_6. Moreover, there is also a sudden increase of Hg···O distance at $n = 6$. Thus $HgCl_2\cdots[O(CH_3)_2]_5$ should be the most stable complex. Differently, $HgCl_2\cdots[S(CH_3)_2]_4$ is the most stable one due to the larger size of S. Such a spodium bond in $HgCl_2\cdots L_n$ complexes is very different from that in $SpX_2L_2\cdots L$ complexes in ref. 53.

4. Conclusion

In summary, we theoretically investigated the linear coordinated spodium bonds in $HgCl_2\cdots L$ (L = ClR, SR_2, PR_3 families) dimers. It was shown that the nature of the spodium bond is the coexistence of the coulombic and covalent interaction. The fact that the trend of the natural charges of the donor atom is opposite to that of the binding energies, together with the deviation of Cl-Hg-Cl angle, supports the presence of covalent interactions, where electrons transfer from donors to unoccupied orbitals of mercury. Besides, $HgCl2\cdots P(CH_3)_3$ dimer is an exception with the largest binding energy and deviation degree, indicating the strongest covalent interaction. ELF and LOL and AdNDP analyses further confirm the existence of covalent interaction and the strongest one lying in $HgCl2\cdots P(CH_3)_3$ dimer. The contribution of charge transfer is very little. In short, the complete picture of weak intermolecular interactions in the linear coordinated spodium bond of

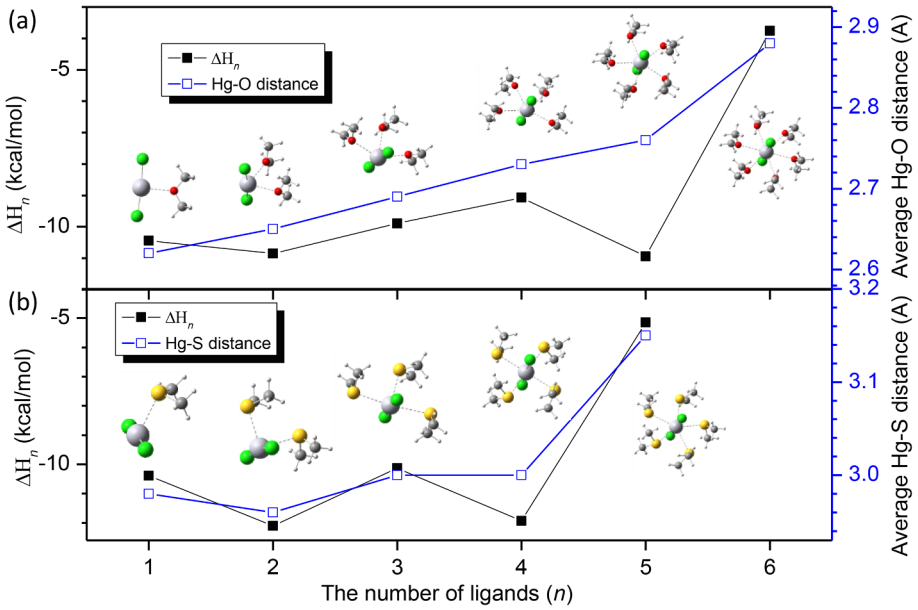

Fig. 9. ΔH_n (kcal/mol) and average Hg···L distance (Å) as a function of the number of ligands (n) at the M06-2x/def2qzvp level: (a) L = $O(CH_3)_2$; (b) L = S $(CH_3)_2$. ΔH_n = $E(HgCl_2\cdots L_n)$ – $E(HgCl_2\cdots L_{n-1})$ –E(L).

Hg elements contains both coulombic and covalent interactions, no one playing the sole role.

CRediT authorship contribution statement

Tao Xia: Software, Writing - original draft. **Dan Li:** Methodology, Writing - review & editing. **Longjiu Cheng:** Supervision.

Declaration of Competing Interest

The authors declare that they have no known competing financial interests or personal relationships that could have appeared to influence the work reported in this paper.

Acknowledgements

This work is financed by the National Natural Science Foundation of China (21873001), and by the Foundation of Distinguished Young Scientists of Anhui Province. The calculations were carried out at the High-Performance Computing Center of Anhui University.

Appendix A. Supplementary data

Supplementary data to this article can be found online at https://doi.org/10.1016/j.chemphys.2020.110978.

References

[1] S. Scheiner, CrystEngComm 15 (16) (2013) 3119–3124.
[2] J. Thirman, E. Engelage, S.M. Huber, M. Head-Gordon, Phys. Chem. Chem. Phys. 20 (2) (2018) 905–915.
[3] C.Z. Liu, S. Koppireddi, H. Wang, D.-W. Zhang, Z.T. Li, Angew. Chem. Int. Ed. 58 (1) (2019) 226–230.
[4] M.E. Wolf, B. Zhang, J.M. Turney, H.F. Schaefer III, Phys. Chem. Chem. Phys. 21 (11) (2019) 6160–6170.
[5] D.M. Ivanov, A.S. Novikov, I.V. Ananyev, Y.V. Kirina, V.Y. Kukushkin, Chem. Commun. 52 (32) (2016) 5565–5568.
[6] S. Scheiner, Faraday Discuss. 203 (2017) 213–226.
[7] J. Manuel Guevara-Vela, D. Ochoa-Resendiz, A. Costales, R. Hernandez-Lamoneda, A. Martin Pendas, ChemPhysChem 19 (19) (2018) 2512–2517.
[8] R. Sedlak, M.H. Kolar, P. Hobza, J. Chem. Theory Comput. 11 (10) (2015) 4727–4732.
[9] S. Scheiner, J. Lu, Chem. Eur. J. 24 (32) (2018) 8167–8177.
[10] S. Scheiner, CrystEngComm 21 (18) (2019) 2875–2883.
[11] A.C. Legon, Phys. Chem. Chem. Phys. 12 (28) (2010) 7736–7747.
[12] A. Bauza, A. Frontera, Crystals 6 (3) (2016) 26.
[13] A. Bauza, A. Frontera, Phys. Chem. Chem. Phys. 18 (47) (2016) 32155–32159.
[14] M. Breugst, D. von der Heiden, J. Schmauck, Synthesis-Stuttgart 49 (15) (2017) 3224–3236.
[15] S. Chandra, A. Bhattacharya, J. Phys. Chem. A 120 (51) (2016) 10057–10071.
[16] V.R. Mundlapati, D.K. Sahoo, S. Bhaumik, S. Jena, A. Chandrakar, H.S. Biswal, Angew. Chem. Int. Ed. 57 (50) (2018) 16496–16500.
[17] P. Politzer, J.S. Murray, T. Clark, J. Mol. Model. 21 (3) (2015) 52.
[18] C. Wang, L. Guan, D. Danovich, S. Shaik, Y. Mo, J. Comput. Chem. 37 (1) (2016) 34–45.
[19] C. Zhu, L. Fang, Macromol. Rapid Commun. 39 (2) (2018) 1700241.
[20] Y. Wang, L. Tang, Prog. Chem. 19 (5) (2007) 769–778.
[21] F. Weinhold, R.A. Klein, Angew. Chem. Int. Ed. 54 (9) (2015) 2600–2602.
[22] J. Elguero, I. Alkorta, J.E. Del Bene, Mol. Phys. 112 (1) (2014) 107–116.
[23] C. Chen, W. Li, Y. Song, L. Weng, Acta Phys. Chim. Sin. 27 (6) (2011) 1372–1378.
[24] H.R. Masoodi, S. Bagheri, M. Ranjbar, Mol. Phys. 114 (23) (2016) 3464–3474.
[25] C.S. Wang, X.J. Qi, Y.G. Ma, Z.Z. Yang, Chem. J. Chinese U. 25 (6) (2004) 1111–1114.
[26] Q. Li, X. Xu, T. Liu, B. Jing, W. Li, J. Cheng, B. Gong, J. Sun, Phys. Chem. Chem. Phys. 12 (25) (2010) 6837–6843.
[27] P. Metrangolo, H. Neukirch, T. Pilati, G. Resnati, Acc. Chem. Res. 38 (5) (2005) 386–395.
[28] P. Politzer, P. Lane, M.C. Concha, Y. Ma, J.S. Murray, J. Mol. Model. 13 (2) (2007) 305–311.
[29] S. Benz, J.L. Lopez-Andarias, J. Mareda, N. Sakai, S. Matile, Angew. Chem. Int. Ed. 56 (3) (2017) 812–815.
[30] V. Oliveira, D. Cremer, E. Kraka, J. Phys. Chem. A 121 (36) (2017) 6845–6862.
[31] S.P. Thomas, V. Kumar, K. Alhameedi, T.N.G. Row, Chem. Eur. J. 25 (14) (2019) 3591–3597.
[32] W. Wang, H. Zhu, S. Liu, Z. Zhao, L. Zhang, J. Hao, Y. Wang, J. Am. Chem. Soc. 141 (23) (2019) 9175–9179.
[33] P. Wonner, A. Dreger, L. Vogel, E. Engelage, S.M. Huber, Angew. Chem. Int. Ed. 58 (47) (2019) 16923–16927.
[34] P. Wonner, L. Vogel, M. Dueser, L. Gomes, F. Kniep, B. Mallick, D.B. Werz, S.M. Huber, Angew. Chem. Int. Ed. 56 (39) (2017) 12009–12012.
[35] L.M. Lee, M. Tsemperouli, A.I. Poblador-Bahamonde, S. Benz, N. Sakai, K. Sugihara, S. Matile, J. Am. Chem. Soc. 141 (2) (2019) 810–814.
[36] A. Bauzá, D. Quiñonero, P.M. Deyà, A. Frontera, CrystEngComm 15 (16) (2013) 3137–3144.
[37] S. Benz, A.I. Poblador-Bahamonde, N. Low-Ders, S. Matile, Angew. Chem. Int. Ed. 57 (19) (2018) 5408–5412.
[38] S. Scheiner, M. Michalczyk, W. Zierkiewicz, Chem. Phys. 524 (2019) 55–62.
[39] A.C. Legon, Phys. Chem. Chem. Phys. 19 (23) (2017) 14884–14896.
[40] R. Vangara, K. Stoltzfus, M.R. York, F. van Swol, D.N. Petsev, Mater. Res. Express 6 (8) (2019) 086331.
[41] J.F. Li, K.C. Wen, W.D. He, X.N. Wang, W.Q. Lu, P.F. Yan, Y.Q. Song, H.L. Lu, X. Lin, J.H. Dickerson, Chin. Phys. B 23 (5) (2014) 1674–11056.
[42] J.W. Gilliland, K. Yokoyama, W.T. Yip, Chem. Mater. 16 (20) (2004) 3949–3954.
[43] O. Mustafa, J. Phys. A-Math. Theor. 44 (35) (2011) 355303.
[44] M.H. Kolar, P. Hobza, Chem. Rev. 116 (9) (2016) 5155–5187.
[45] P. Politzer, J.S. Murray, T. Clark, Phys. Chem. Chem. Phys. 15 (27) (2013) 11178–11189.
[46] T. Clark, M. Hennemann, J.S. Murray, P. Politzer, J. Mol. Model. 13 (2) (2007) 291–296.
[47] O. Hassel, Science 170 (1970) 497–502.
[48] A.E. Reed, F. Weinhold, R. Weiss, J. Macheleid, J. Phys. Chem. 89 (1985)

2688–2694.
[49] S.M. Huber, J.D. Scanlon, E. Jimenez-Izal, J.M. Ugalde, I. Infante, Phys. Chem. Chem. Phys. 15 (25) (2013) 10350–10357.
[50] S.W. Robinson, C.L. Mustoe, N.G. White, A. Brown, A.L. Thompson, P. Kennepohl, P.D. Beer, J. Am. Chem. Soc. 137 (1) (2015) 499–507.
[51] K.E. Riley, P. Hobza, Phys. Chem. Chem. Phys. 15 (41) (2013) 17742–17751.
[52] G.R. Desiraju, P.S. Ho, L. Kloo, A.C. Legon, R. Marquardt, P. Metrangolo, P. Politzer, G. Resnati, K. Rissanen, Pure Appl. Chem. 85 (8) (2013) 1711–1713.
[53] A. Bauza, I. Alkorta, J. Elguero, T.J. Mooibroek, A. Frontera, Angew. Chem. Int. Ed. (2020), https://doi.org/10.1002/anie.202007814.
[54] S. Biering, P. Schwerdtfeger, J. Chem. Phys. 136 (3) (2012) 034504.
[55] H. Cheng, L. Cheng, Comput. Theor. Chem. 1060 (2015) 36–42.
[56] Y. Zhao, D.G. Truhlar, Acc. Chem. Res. 41 (2) (2008) 157–167.
[57] M. J. T. Frisch, G. W.; Schlegel, H. B.; Scuseria, G. E.; Robb, M. A.; Cheeseman, J. R.; Montgomery, J. A.; Jr.; Vreven, T.; Kudin, K. N.; Burant, J. C.; Millam, J. M.; Iyengar, S. S.; Tomasi, J.; Barone, V.; Mennucci, B.; Cossi, M.; Scalmani, G.; Rega, N. ; Petersson, G. A.; Nakatsuji, H.; Hada, M.; Ehara, M.; Toyota, K.; Fukuda, R.; Hasegawa, J.; Ishida, M.; Nakajima, T.; Honda, Y.; Kitao, O.; Nakai, H.; Klene, M.; Li, X.; Knox, J. E.; Hratchian, H. P.; Cross, J. B.; Bakken, V.; Adamo, C.; Jaramillo, J.; Gomperts, R.; Stratmann, R. E.; Yazyev, O.; Austin, A. J.; Cammi, R.; Pomelli, C.; Ochterski, J. W.; Ayala, P. Y.; Morokuma, K.; Voth, G. A.; Salvador, P.; Dannenberg, J. J.; Zakrzewski, V. G.; Dapprich, S.; Daniels, A. D.; Strain, M. C.; Farkas, O.; Malick, D. K.; Rabuck, A. D.; Raghavachari, K.; Foresman, J. B.; Ortiz, J. V.; Cui, Q.; Baboul, A. G.; Clifford, S.; Cioslowski, J.; Stefanov, B. B.; Liu, G.; iashenko, A.; Piskorz, P.; Komaromi, I.; Martin, R. L.; Fox, D. J.; Keith, T.; Al-Laham, M. A.; Peng, C. Y.; Nanayakkara, A.; Challacombe, M.; Gill, P. M. W.; Johnson, B.; Chen, W.; Wong, M. W.; Gonzalez, C.; Pople, J. A., Gaussian 09. Wallingford: 2009.
[58] A.E. Reed, F. Weinhold, J. Chem. Phys. 78 (1982) 4066–4073.
[59] A.E. Reed, R.B. Weinstock, F. Weinhold, J. Chem. Phys. 83 (2) (1985) 735–746.
[60] F. Weinhold, J. Comput. Chem. 33 (30) (2012) 2363–2379.
[61] F. Weigend, R. Ahlrichs, Phys. Chem. Chem. Phys. 7 (2005) 3297–3305.
[62] B. Silvi, A. Savin, Nature 371 (1994) 683–686.
[63] H. Jacobsen, Can. J. Chem. 86 (7) (2008) 695–702.
[64] T. Lu, F. Chen, J. Comput. Chem. 33 (5) (2012) 580–592.
[65] E. Johnson, S. Keinan, P. Mori-Sanchez, J. Contreras-Garcia, A. Cohen, W. Yang, J. Am. Chem. Soc. 132 (2010) 6498–6506.
[66] W. Humphrey, A. Dalke, K. Schulten, J. Mol. Graph. 14 (1996) 33–38.
[67] D.Y. Zubarev, A.I. Boldyrev, Phys. Chem. Chem. Phys. 10 (34) (2008) 5207–5217.
[68] R. Wysokinski, W. Zierkiewicz, M. Michalczyk, S. Scheiner, Chem. Phys. Chem. 21 (2020) 1–8.
[69] T. Ziegler, A. Rauk, Inorg. Chem. 18 (1979) 1755–1759.
[70] T. Ziegler, A. Rauk, Theoret. Chim. Acta (Berl.) 46 (1977) 1–10.
[71] A. Michalak, M. Mitoraj, T. Ziegler, J. Phys. Chem. A 112 (2008) 1933–1939.
[72] M. Mitoraj, A. Michalak, J. Mol. Model. 13 (2) (2007) 347–355.
[73] ADF2008.01, SCM, Theoretical Chemistry, Vrije Universiteit, Amsterdam, The Netherlands. http://www.scm.com.
[74] K. Szalewicz, Wileys Comput. Mol. Sci. 2 (2012) 254–272.
[75] R.M. Parrish, L.A. Burns, D.G.A. Smith, A.C. Simmonett, A.E. DePrince III, E.G. Hohenstein, U. Bozkaya, A.Y. Sokolov, R. Di Remigio, R.M. Richard, J.F. Gonthier, A.M. James, H.R. McAlexander, A. Kumar, M. Saitow, X. Wang, B.P. Pritchard, V. Prakash, H.F. Schaefer III, K. Patkowski, R.A. King, E.F. Valeev, F.A. Evangelista, J.M. Turney, T.D. Crawford, C.D. Sherrill, J. Chem. Theory Comput. 13 (2017) 3185–3197.
[76] P. Matczak, Mol. Phys. 115 (2017) 364–378.
[77] M. Palusiak, J. Mol. Struct. – Theochem. 945 (2010) 89–92.
[78] P. Politzer, J.S. Murray, T. Clark, Phys. Chem. Chem. Phys. 15 (2013) 11178–11189.
[79] Z. Wang, Y. Liu, B. Zheng, F. Zhou, Y. Jiao, Y.X. Liu, T. Lu, J. Chem. Phys. 148 (2018) 194106.